Interaction of Akt-Phosphorylated Ataxin-1 with 14-3-3 Mediates Neurodegeneration in Spinocerebellar Ataxia Type 1

Hung-Kai Chen,[1,4] Pedro Fernandez-Funez,[1]
Summer F. Acevedo,[6] Yung C. Lam,[3]
Michael D. Kaytor,[5] Michael H. Fernandez,[4]
Alastair Aitken,[8] Efthimios M.C. Skoulakis,[6,7]
Harry T. Orr,[5] Juan Botas,[1] and Huda Y. Zoghbi[1,2,3,4,9]
[1]Department of Molecular and Human Genetics
[2]Department of Pediatrics
[3]Division of Neuroscience
[4]Howard Hughes Medical Institute
Baylor College of Medicine
One Baylor Plaza
Houston, Texas 77030
[5]Institute of Human Genetics
University of Minnesota
Mayo Mail Code 206
Minneapolis, Minnesota 55455
[6]Department of Biology and Program in Genetics
Texas A&M University
College Station, Texas 77843
[7]Institute of Molecular Biology and Genetics
BSRC "A. Fleming"
16672 Vari, Greece
[8]Division of Biomedical and Clinical Laboratory
  Sciences
University of Edinburgh
Edinburgh
EH8 9XD, Scotland
United Kingdom

Summary

Spinocerebellar ataxia type 1 (SCA1) is one of several neurological disorders caused by a CAG repeat expansion. In SCA1, this expansion produces an abnormally long polyglutamine tract in the protein ataxin-1. Mutant polyglutamine proteins accumulate in neurons, inducing neurodegeneration, but the mechanism underlying this accumulation has been unclear. We have discovered that the 14-3-3 protein, a multifunctional regulatory molecule, mediates the neurotoxicity of ataxin-1 by binding to and stabilizing ataxin-1, thereby slowing its normal degradation. The association of ataxin-1 with 14-3-3 is regulated by Akt phosphorylation, and in a *Drosophila* model of SCA1, both 14-3-3 and Akt modulate neurodegeneration. Our finding that phosphatidylinositol 3-kinase/Akt signaling and 14-3-3 cooperate to modulate the neurotoxicity of ataxin-1 provides insight into SCA1 pathogenesis and identifies potential targets for therapeutic intervention.

Introduction

Spinocerebellar ataxia type 1 (SCA1) is an autosomal dominant neurodegenerative disease caused by the expansion of a CAG repeat that produces an abnormally long polyglutamine tract in the ataxin-1 protein. At least

[9]Correspondence: hzoghbi@bcm.tmc.edu

eight other inherited neurodegenerative diseases, including Huntington's disease, are caused by a similar pathogenic mechanism (reviewed in Zoghbi and Orr, 2000; Nakamura et al., 2001). In each case, the length of the CAG repeat tract correlates with disease severity: more repeats produce more severe symptoms with an earlier age of onset. The expanded polyglutamine tract appears to confer a toxic gain-of-function that intensifies with longer repeats.

Another feature common to the polyglutamine diseases studied so far (as well as several other neurodegenerative disorders) is aberrant protein deposition: mutant polyglutamine proteins have a strong tendency to accumulate and eventually form aggregates in neurons (Zoghbi and Orr, 2000; Kaytor and Warren, 1999). We have proposed that the polyglutamine expansion alters the protein's conformation in such a way as to make the protein recalcitrant to proteasomal degradation (Cummings et al., 1998). In the case of ataxin-1, even the unexpanded protein can produce pathology if expressed at sufficiently high levels (Fernandez-Funez et al., 2000), which suggests that wild-type ataxin-1 might have more than one stable conformation — and that one or more of these alternate conformations is toxic if it becomes abundant. Support for this idea has come from the study of α-synuclein, whose accumulation causes Parkinson's Disease (PD). Although rare cases of familial PD are caused by point mutations in α-synuclein, most PD is associated with abnormal accumulation of *wild-type* α-synuclein (Dawson et al., 2002). These observations raise several important questions: what factors contribute to the altered protein conformation? How exactly do misfolded proteins induce neuronal dysfunction and degeneration? And what factors modulate their toxicity?

The subcellular localization of the polyglutamine protein, the ratio of the polyglutamine tract to the host protein, and native protein sequences flanking the CAG repeat all affect the toxicity of polyglutamine proteins (Zoghbi and Botas, 2002). Protein modifications such as phosphorylation may also have an effect: in Alzheimer's disease (AD), for example, brain dysfunction and degeneration are linked to the accumulation of the neurofibrillary tangles that are highly enriched in the hyperphosphorylated forms of the microtubule-associated protein tau (Lee et al., 2001). Enhanced phosphorylation of tau by glycogen synthase kinase 3β (GSK3β) induces filamentous tau inclusions and accelerates tau-induced neurodegeneration in transgenic flies (Jackson et al., 2002) and mice (Lucas et al., 2001). Given these findings, we enquired whether protein phosphorylation might play a role in SCA1 pathogenesis as well.

Recently, Emamian and colleagues demonstrated that ataxin-1 is phosphorylated at serine 776 (S776) and that substitution of this S776 residue with alanine (A776) greatly diminishes the ability of mutant ataxin-1 to aggregate (Emamian et al., 2003). These results suggest that a serine at position 776 of ataxin-1 plays a role in SCA1 pathogenesis. Because this serine is normally phosphorylated, we speculated that S776 phosphoryla-
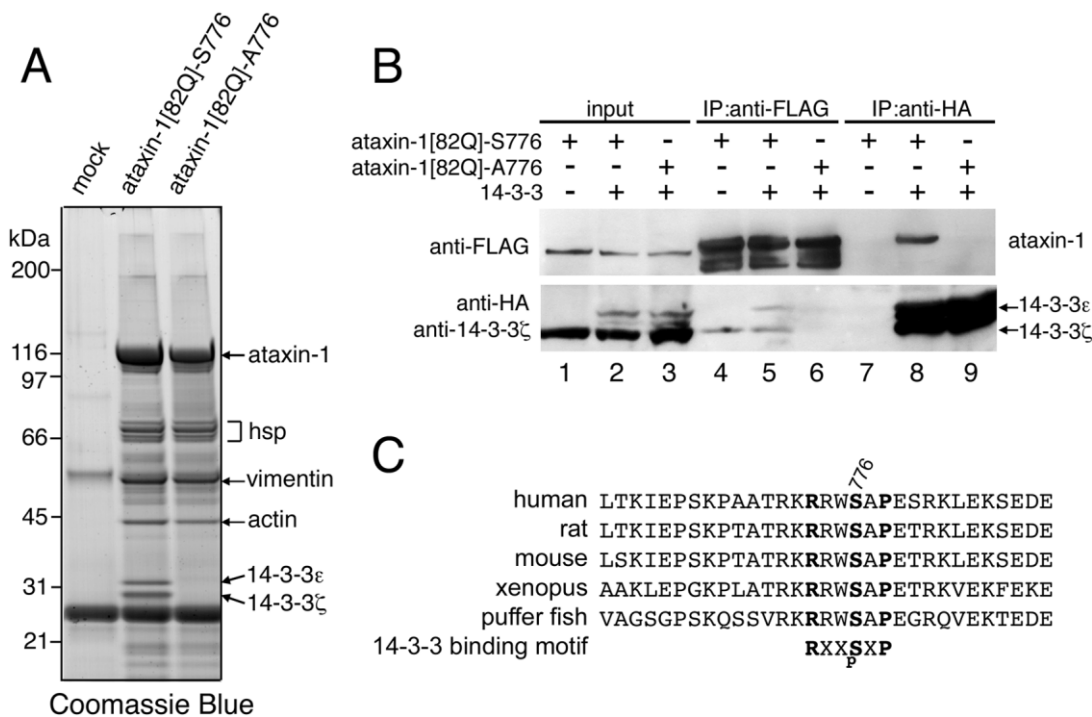
Figure 1. Ataxin-1 Interacts with 14-3-3

(A) Lysates from COS1 cells transfected with FLAG-ataxin-1[82Q] (S776 or A776) or mock control were immunoprecipitated by anti-FLAG antibodies. 14-3-3ζ and 14-3-3ε interact specifically with ataxin-1[82Q]-S776. (hsp: heat shock proteins)

(B) Association of ataxin-1 and 14-3-3 requires S776. Lysates of COS1 cells cotransfected with FLAG-tagged ataxin-1[82Q] (S776 or A776) or bi-cistronic HA-14-3-3ε and myc-14-3-3ζ (pIRES-HA-14-3-3ε/myc-14-3-3ζ) were immunoprecipitated by either anti-FLAG or anti-HA antibodies. The lysates (input) and immunoprecipitates were analyzed by immunoblotting with anti-FLAG or mixtures of anti-HA and anti-14-3-3ζ antibodies.

(C) Ataxin-1 homologs from different species share a consensus 14-3-3 binding motif.

tion might modify ataxin-1 neurotoxicity by regulating its protein-protein interactions. To test this hypothesis, we sought to identify proteins that interact with ataxin-1-S776 but not ataxin-1-A776, to identify the kinase that phosphorylate S776 in ataxin-1, and examine the effects of these factors on SCA1 pathogenesis.

Results

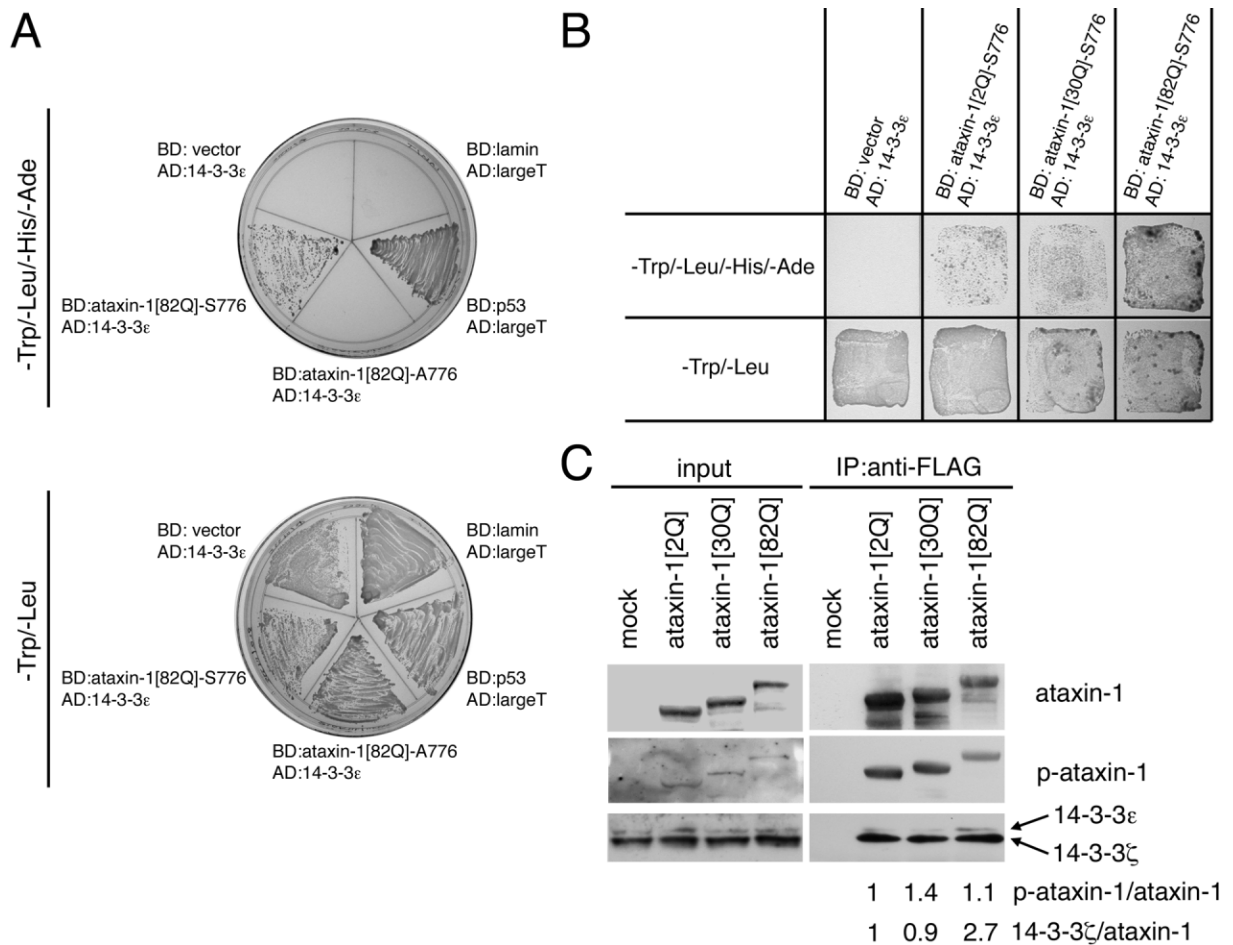### Ataxin-1 Interacts with 14-3-3

To identify proteins that preferentially interact with ataxin-1-S776, we performed immunoprecipitation on cell lysates from COS1 cells transiently transfected with FLAG-tagged ataxin-1 containing 82 glutamines (82Q) and either a serine (ataxin-1[82Q]-S776) or an alanine (ataxin-1[82Q]-A776) at position 776. SDS-PAGE analysis revealed several polypeptides that coprecipitated with ataxin-1 (Figure 1A). These proteins were purified and subjected to trypsin digestion followed by mass spectrometry. A number of chaperones were detected in the immunoprecipitates of both ataxin-1[82Q]-S776 and ataxin-1[82Q]-A776, including inducible Hsp70, Hsc70, Hsp40, and BiP/GRP78 (Figure 1A, and data not shown), which suggests that both forms of ataxin-1[82Q] adopt misfolded conformations readily recognized by heat shock proteins. β-actin and vimentin were also detected in the immunoprecipitates of both ataxin-1 variants. Interestingly, two proteins with apparent mo-

lecular masses of 30 and 28 kDa coprecipitated only with ataxin-1[82Q]-S776. The mass values of their derived peptides matched the ε and ζ isoforms of 14-3-3, a protein family of multifunctional regulatory molecules (Fu et al., 2000).

To verify the interaction between ataxin-1 and 14-3-3, we performed immunoprecipitation on lysates from COS1 cells transfected with FLAG-tagged ataxin-1 and a plasmid bi-cistronically expressing HA-tagged 14-3-3ε and myc-tagged 14-3-3ζ proteins (Figure 1B). Ataxin-1[82Q]-S776 immunoprecipitated both 14-3-3ζ (lanes 4 and 5, Figure 1B) and 14-3-3ε (lane 5, Figure 1B), but ataxin-1[82Q]-A776 failed to pull down any of the 14-3-3 proteins (lane 6, Figure 1B). Conversely, 14-3-3 immunoprecipitated only ataxin-1[82Q]-S776 (compare lanes 8 and 9, Figure 1B). Complex formation between ataxin-1 and 14-3-3 in vivo thus requires the serine residue at position 776 in ataxin-1. The sequence of ataxin-1 (amino acids 773-778) is similar to a consensus 14-3-3 binding motif (Fu et al., 2000) that comprises an essential phosphoserine residue flanked by an arginine and proline (Figure 1C). This motif is present in ataxin-1 homologs of different species, suggesting that the ataxin-1/14-3-3 interaction has been evolutionarily conserved.

To probe whether the ataxin-1/14-3-3 interaction is direct or indirect, we performed a yeast two-hybrid screen using an evolutionarily conserved C-terminal fragment of ataxin-1 (amino acids 529–816, denoted "ataxin-1C288", which contains the postulated 14-3-3

Figure 2. 14-3-3 Interacts Directly with Ataxin-1 and Binds Most Strongly to the Expanded Form

(A and B) Ataxin-1[82Q]-S776, but not ataxin-1[82Q]-A776 interacts with 14-3-3ε (A) in a yeast two-hybrid system. Double transformants of ataxin-1[82Q]-S776/14-3-3ε grew faster than those of either ataxin-1[2Q]-S776/14-3-3ε or ataxin-1[30Q]-S776/14-3-3ε on -Trp/-Leu/-His/-Ade medium but grew similarly on –Trp/-Leu medium (B). BD and AD are DNA binding and activation domains, respectively.

(C) 14-3-3 binds most strongly to expanded ataxin-1. Lysates of COS1 cells transfected with FLAG-tagged ataxin-1 (2Q, 30Q, or 82Q) or a control plasmid (mock) were immunoprecipitated with anti-FLAG. The input and immunoprecipitates were resolved in SDS-PAGE, and immunoblotted with anti-FLAG, anti-ataxin-1-pS776, or mixtures of anti-14-3-3ε and anti-14-3-3ζ antibodies. Anti-14-3-3ε antibodies give weaker signals than anti-14-3-3ζ due to a lower affinity. 14-3-3 associates most strongly with ataxin-1[82Q] based on the amount immunoprecipitated relative the total amount of soluble ataxin-1 that can be immunoprecipitated. Ataxin-1 variants were phosphorylated similarly as revealed by the relative signal ratio of S776-phosphorylated ataxin-1 (p-ataxin-1) to total ataxin-1. Normalized quantification is shown.

binding motif). 14-3-3 (β and ε) was the most frequently identified interactor (data not shown). When we examined the ability of full-length ataxin-1 to interact with 14-3-3 in the yeast two-hybrid system, we found that only ataxin-1[82Q]-S776 (but not A776) interacted with the ε, ζ, and β isoforms of 14-3-3 (Figure 2A, and data not shown).

To determine whether ataxin-1 interacts with different isoforms of 14-3-3 in vivo, we used isoform-specific antibodies to detect 14-3-3 proteins in ataxin-1 immunoprecipitates from Neuro2A cells transfected with ataxin-1[82Q]-S776. Several 14-3-3 isoforms, including ε, ζ, η, γ, and β, were detectable in the immunocomplex of ataxin-1 (data not shown).

14-3-3 Associates Most Strongly with Expanded Ataxin-1

Because the ataxin-1C288 fragment that does not contain the polyglutamine tract can interact with 14-3-3

proteins in yeast, the polyglutamine tract itself is not required for ataxin-1/14-3-3 interactions. Nonetheless, double transformants of expanded ataxin-1[82Q] and 14-3-3 grew slightly faster than those of unexpanded ataxin-1 (2Q or 30Q) and 14-3-3 on medium lacking leucine, tryptophan, histidine, and adenine (Figure 2B). This observation suggests that 14-3-3 binds more strongly to mutant ataxin-1. To test the effect of polyglutamine tract length on ataxin-1/14-3-3 binding, we transfected COS1 cells with constructs encoding ataxin-1 bearing either 2Q, 30Q, or 82Q. Although the amounts of immunoprecipitated ataxin-1 decreased with longer glutamine tracts because of lower protein solubility, similar amounts of 14-3-3 coimmunoprecipitated with each protein (Figure 2C); i.e., the relative amount of immunoprecipitated 14-3-3 was highest in cells transfected with ataxin-1[82Q]. These differences could not be attributed to changes in the endogenous levels of 14-3-3 proteins, which did not differ in the transfected cells (Figure 2C,

input). Because 14-3-3 binding is usually phosphorylation-dependent, we speculated that ataxin-1 with polyglutamine tracts of variable lengths might be phosphorylated differentially. We tested this hypothesis using an antibody, PN1168, that specifically recognizes ataxin-1 with a phosphoserine at position S776 (Emamian et al., 2003; denoted as anti-ataxin-1-pS776). Immunoblotting with this antibody showed that ataxin-1 proteins were phosphorylated similarly irrespective of polyglutamine tract length (Figure 2C). Therefore, the differential abilities of ataxin-1 2Q, 30Q, and 82Q to interact with 14-3-3 are not attributable to different levels of phosphorylation. Rather, it is likely that expanded ataxin-1[82Q] attains a certain conformation that is more favorable for 14-3-3 binding.

14-3-3 Stimulates Ataxin-1 Inclusion Formation

We examined the subcellular localization of ataxin-1 and 14-3-3 in COS1 cells. In cells transfected with 14-3-3 alone, 14-3-3 distributed to both the cytoplasm and nucleoplasm (Figure 3A, arrowhead), as observed previously (Brunet et al., 2002). In cells transfected with both proteins, 14-3-3 was recruited to the nuclear aggregates formed by ataxin-1 (Figure 3A, arrows). Could 14-3-3 influence ataxin-1's ability to form inclusions or become sequestered itself in aggregates and thus be diverted from its normal functions? To answer these questions we sought to determine whether 14-3-3 modulates ataxin-1's ability to form inclusions or if 14-3-3 overexpression influences ataxin-1-induced neurodegeneration.

A majority of COS1 cells (over 70%) transiently transfected with ataxin-1[82Q]-S776 develop numerous nuclear inclusions (Cummings et al., 1998), whereas cells transfected with ataxin-1[82Q]-A776, which is defective in 14-3-3 binding, show ataxin-1[82Q]-A776 distributed throughout the nucleoplasm, with fewer than 10% of transfectants forming inclusions (Emamian et al., 2003). We tested the effects of different levels of 14-3-3 on ataxin-1 inclusion formation. To achieve a condition of 14-3-3 overexpression, we cotransfected COS1 cells with 14-3-3 and ataxin-1 at a higher molar ratio (5:1, 14-3-3 to ataxin-1) than the 1:1 ratio used earlier (cf., Figure 3A). 14-3-3 overexpression had little effect on ataxin-1[82Q]-A776, which remained evenly distributed in the nucleoplasm of most transfectants (Figure 3B, panels 4 to 6). Rare ataxin-1[82Q]-A776 aggregates were detected in some transfectants, but in these cells, 14-3-3 was evenly distributed and did not redistribute to the site of the inclusions (Figure 3B, panels 4 to 6, arrowhead). Transfectants expressing high levels of 14-3-3 along with ataxin-1[82Q]-S776, however, bore numerous large inclusions (Figure 3B, panels 1 to 3, arrows). These inclusions frequently occupied more than half of the nuclear volume and expelled chromatin to the edge of nuclei—such aggravated inclusion formation is never seen when ataxin-1[82Q]-S776 is transfected alone (data not shown; Cummings et al., 1998).

14-3-3 Increases Steady-State Levels of Ataxin-1

We hypothesized that the ability of 14-3-3 to stimulate ataxin-1 inclusion formation resulted from its ability to stabilize the mutant protein. To test this hypothesis,

we transfected HeLa cells with 14-3-3 and ataxin-1. As predicted, 14-3-3 overexpression greatly increased the steady-state levels of ataxin-1[82Q]-S776, but not ataxin-1[82Q]-A776 (Figure 3C); this effect was much more pronounced with expanded ataxin-1[82Q]-S776 than with ataxin-1[2Q]-S776. This result is consistent with our finding that ataxin-1[82Q] has a higher binding affinity to 14-3-3 (Figures 2B and 2C). More importantly, we found that 14-3-3 must interact directly with ataxin-1 to stabilize it. Ataxin-1[82Q]-A776, which is defective in the 14-3-3 binding, resisted stabilization by 14-3-3 (Figure 3C). The differential effects of 14-3-3 on ataxin-1 variants ruled out the possibility that 14-3-3 might generally enhance the transcription of the transgenes, since all of them are driven by the same promoter. These data suggest that 14-3-3 modulates mutant ataxin-1 toxicity by retarding ataxin-1 degradation.

14-3-3 Aggravates Neurodegeneration in SCA1 Flies

To investigate the in vivo effects of 14-3-3 on ataxin-1-induced neurodegeneration in our fly model of SCA1 (Fernandez-Funez et al., 2000), we generated double transgenic flies expressing ataxin-1[82Q] and *Drosophila* 14-3-3ε (*d14-3-3ε*) using the GAL4/UAS system, in which transgenic expression is directed to the retina by the *gmr-GAL4* driver (see Fernandez-Funez et al., 2000).

To increase our chances of observing subtle phenotypes, we raised transgenic flies at 23°C to allow a lower level of ataxin-1[82Q] expression (Fernandez-Funez et al., 2000). Under this condition, transgenic flies expressing ataxin-1[82Q] alone (*SCA1*^{82Q}) displayed a mild degenerative phenotype with a moderate disruption of the regular external lattice, a thinner retina layer, and mildly abnormal rhabdomeres (Figure 4A, panels 2 and 5, and data not shown). Overexpression of d14-3-3ε in flies produces no deleterious effects on its own (data not shown). But *SCA1*^{82Q}/*d14-3-3ε* double transgenic flies had a much more severe phenotype than those expressing ataxin-1[82Q] alone, showing profoundly disordered ommatidia, a thin and disorganized retina layer, and grossly abnormal rhabdomeres (Figure 4A, panels 3 and 6, and data not shown). This aggravated phenotype was observed in *SCA1*^{82Q}/*d14-3-3ε* double transgenic flies derived from different individual weak lines for both transgenes (data not shown). 14-3-3 thus intensifies ataxin-1-induced neurodegeneration in a fly model of SCA1.

14-3-3 Stabilizes Ataxin-1 in SCA1 Flies

Upon breeding different *d14-3-3ε* transgenic lines to *SCA1*^{82Q} flies, a synthetic lethality in the double transgenic animals was reproducibly observed in combinations of lines that have relatively high expression of either *d14-3-3ε* or *SCA1*^{82Q} transgenes (data not shown). While all high-expressing transgenic animals bearing only the *SCA1*^{82Q} or the *d14-3-3ε* transgene develop normally to adulthood, double transgenic animals died in the second to third instar larval stage. This effect is specific to ataxin-1, as we have not observed lethality in flies overexpressing d14-3-3ε in conjunction with other transgenes (data not shown). This result demonstrates a specific interaction between ataxin-1 and d14-3-3ε:
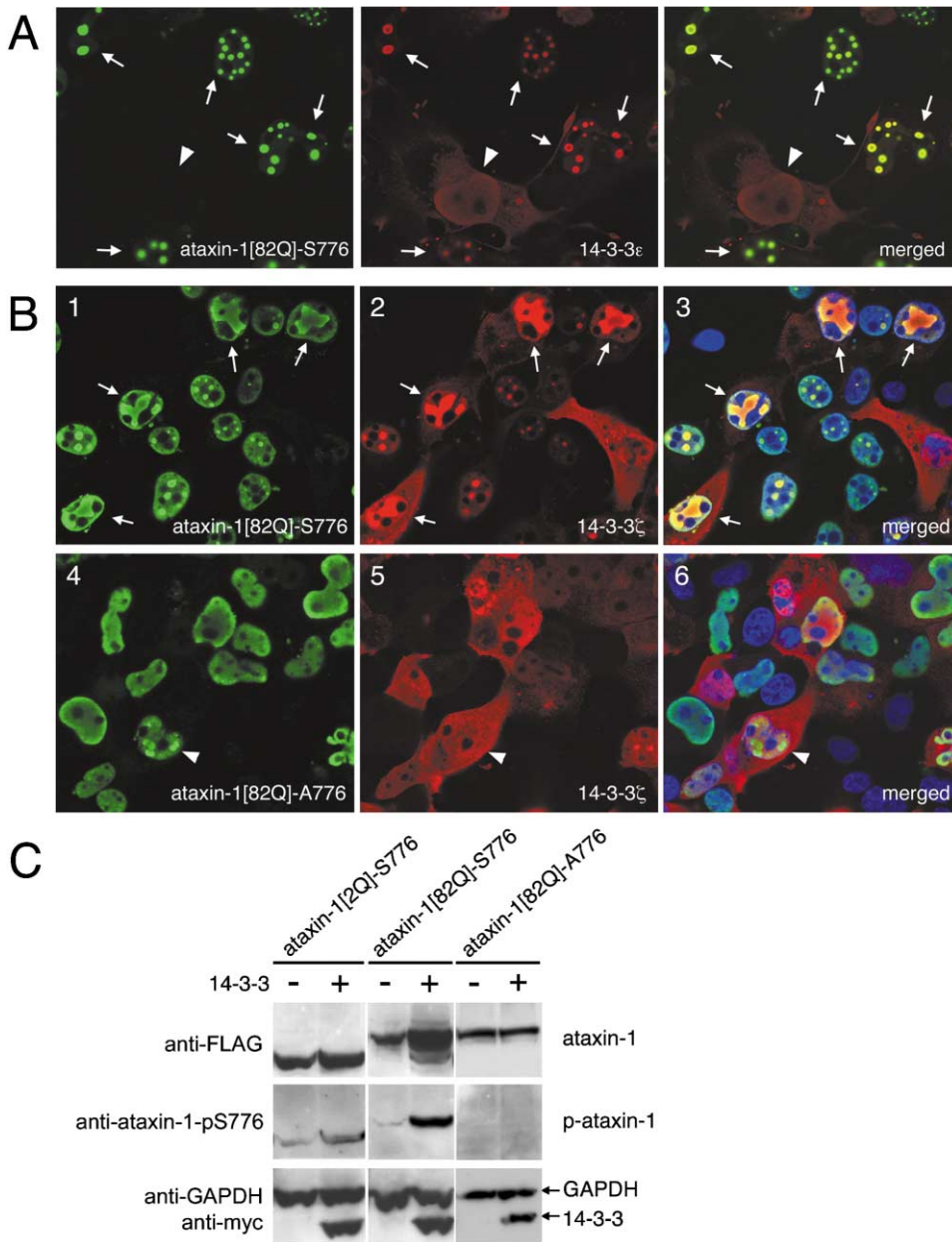
Figure 3. 14-3-3 Stabilizes Ataxin-1 through Their Interactions

(A) COS1 cells were transfected with GFP-ataxin-1[82Q]-S776 and pIRES-HA-14-3-3ε/myc-14-3-3ζ(left and middle panels, respectively). Confocal microscopy analysis revealed that ataxin-1[82Q]-S776 (GFP, green) and 14-3-3ε (anti-HA, red) extensively colocalize (yellow) in double transfectants (arrows in the merged image, right panel). In cells transfected with 14-3-3 alone (arrowhead), 14-3-3 was distributed to the cytoplasm and nucleoplasm. (B) COS1 cells were cotransfected with FLAG- ataxin-1[82Q] (S776; panels 1 to 3 or A776; panels 4 to 6) and myc14-3-3ζ. Double immunofluorescence staining was done using anti-FLAG (green) and anti-myc (red) antibodies, whereas the DNA was counterstained with DAPI (Blue). Huge ataxin-1 inclusions (arrows) form when 14-3-3 is overexpressed with ataxin-1[82Q]-S776. In contrast, ataxin-1[82Q]-A776 was evenly distributed in most cells irrespective of the coexpression of 14-3-3. Nuclear inclusions formed by ataxin-1[82Q]-A776 were present in only a few cells (arrowhead).

(C)14-3-3 overexpression increases steady-state levels of ataxin-1 harboring S776 but not A776. HeLa cells were cotransfected with FLAG-ataxin-1 ([2Q]-S776, [82Q]-S776, or [82Q]-A776) and myc-tagged 14-3-3ζ (+), or a control plasmid (−). Immunoblotting was done with anti-FLAG, anti-ataxin-1-pS776, and mixtures of anti-GAPDH and anti-myc antibodies.

ataxin-1 toxicity was greatly enhanced in animals carrying overexpression alleles of *d14-3-3ε*.

Oddly, this early lethality of *SCA1[82Q]/d14-3-3ε* double transgenic animals occurred even in the absence of *gmr-GAL4* driver. We speculated that the leakage-prone UAS promoter might give rise to low expression of ataxin-1 that gradually accumulates in the presence of leaky d14-3-3ε expression due to the latter's stabilization effect upon ataxin-1. We therefore examined the larvae of *SCA1[82Q]/d14-3-3ε* double transgenic animals
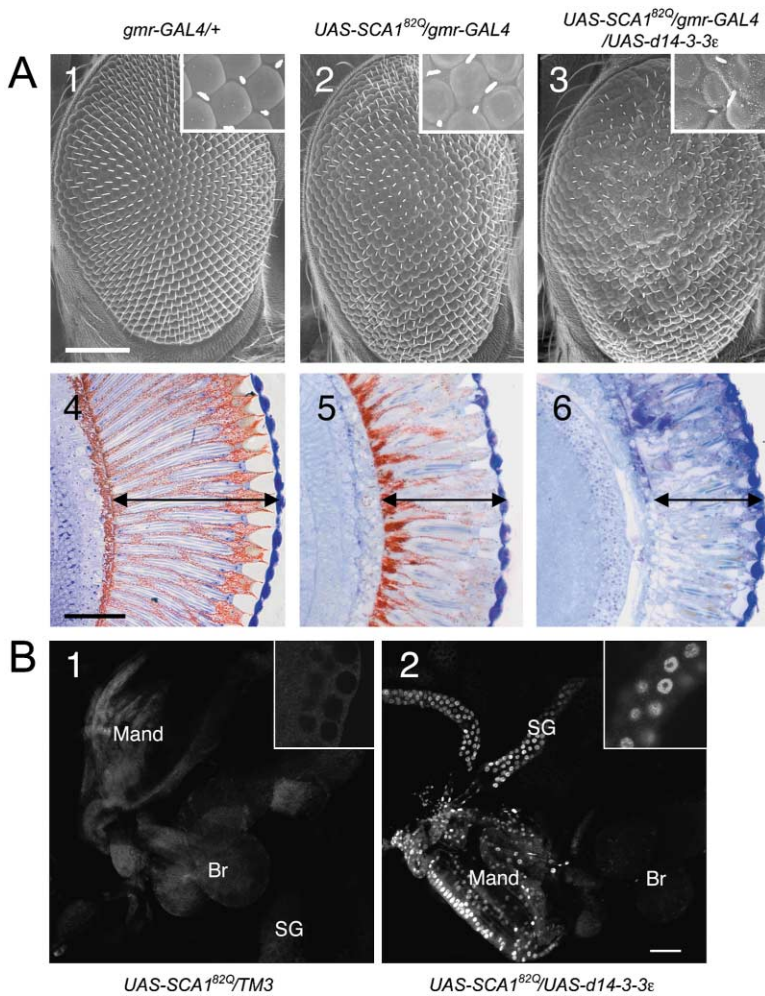
Figure 4. 14-3-3 Stabilizes Mutant Ataxin-1 and Enhances Its Toxicity in Flies

(A) 14-3-3 promotes ataxin-1-induced neuro-degeneration. SEM eye images (panels 1–3) and vertical eye sections (panels 4–6) of a control fly eye (*gmr-GAL4/+*, panels 1 and 4), or transgenic fly eyes expressing mutant ataxin-1 (*UAS-SCA1[82Q][F7]/gmr-GAL4*, panels 2 and 5), or ataxin-1 with *Drosophila* 14-3-3ε (*UAS-SCA1[82Q][F7]/gmr-GAL4/UAS-d14-3-3[9or]*, panels 3 and 6). Insets in panels 1–3 are higher magnification views of ommatidia. Arrows indicate retinal thickness (panels 4–6). Ataxin-1/14-3-3ε double transgenic flies (panels 3 and 6) show severe disruption of external lattice and a thin, disorganized retina. Flies were raised at 23°C. Scale bar: 100 μm (panel 1), 50 μm (panel 4).

(B) Leaky levels of mutant ataxin-1 are dramatically increased in *SCA1[82Q]/d14-3-3ε* double transgenic animals in the absence of a *GAL4* driver. Leaky ataxin-1[82Q] expression was barely detectable in the second instar larvae of animals carrying *SCA1[82Q]* transgene alone (*UAS-SCA1[82Q][N35y]/TM3*, panel 1) but was high in in the mandibles (mand) and salivary glands (SG) of *SCA1[82Q]/d14-3-3ε* animals (*UAS-SCA1[82Q][N35y]/UAS-d14-3-3ε*, panel 2) due to its stabilization. Ataxin-1[82Q] was also detectable in a few brain neurons (Br). Insets show higher magnifications of the salivary glands. Scale bar: 50 μm.

for leaky expression of ataxin-1 in the absence of the GAL4 driver. We found significant amounts of ataxin-1 in many polytenic cells in the mandible and in the salivary glands of *SCA1[82Q]/d14-3-3ε* larvae (Figure 4B, panel 2), while ataxin-1 was barely detectable in larvae carrying the *SCA1[82Q]* transgene alone (Figure 4B, panel 1). This finding is consistent with our observation that coexpression of 14-3-3 with ataxin-1[82Q] in transfected cells leads to the accumulation of ataxin-1[82Q] (Figure 3C). This result also supports the notion that ataxin-1 accumulation due to the stabilizing interaction with 14-3-3 causes the synthetic lethality in *SCA1[82Q]/d14-3-3ε* double transgenic animals.

Ataxin-1 Is a Substrate of Akt Kinase

To determine if the interaction of ataxin-1 and 14-3-3 is regulated by protein phosphorylation at the S776 residue, we sought to identify the kinase that phosphorylates ataxin-1 at S776. We analyzed the sequence of ataxin-1 with a motif search program at the Scansite website (http://scansite.mit.edu; Yaffe et al., 2001) and identified the S776 residue as a putative Akt kinase phosphorylation site. This consensus motif for Akt phosphorylation (RXRXXS) is conserved in ataxin-1 homologs (Figure 1C). To determine whether ataxin-1 is a substrate of Akt kinase, we performed an in vitro phos-

phorylation assay by incubating bacterially expressed glutathione S-transferase-ataxin-1[30Q] fusion protein (GST-ataxin-1) with purified Akt1 kinase in a kinase reaction buffer. As determined by autoradiography for ^{32}P incorporation, GST-ataxin-1, but not a control GST protein, was heavily phosphorylated by Akt1 kinase (Figure 5A). This result suggests that ataxin-1 is indeed a substrate of Akt kinase. In addition, Akt1 phosphorylates ataxin-1 at the S776 residue, since the bacterially expressed ataxin-1 was recognized by anti-ataxin-1-pS776 antibody only after Akt phosphorylation (Figure 5A).

To determine whether ataxin-1 is phosphorylated by Akt in vivo, we cotransfected HeLa cells with ataxin-1[2Q] and either a constitutively active form of Akt1 (CA-Akt) or an inactive dominant-negative form of Akt1 (DN-Akt). We found that CA-Akt induced ataxin-1 phosphorylation while DN-Akt inhibited it (Figure 5B). Interestingly, coexpression of CA-Akt increased the steady-state levels of ataxin-1-S776 but not ataxin-1-A776, while levels of the endogenous 14-3-3 remained unchanged (Figure 5B and data not shown).

Interaction of Ataxin-1 and 14-3-3 Requires Akt Phosphorylation at S776

The importance of Akt phosphorylation for the association of ataxin-1 and 14-3-3 was examined using an in
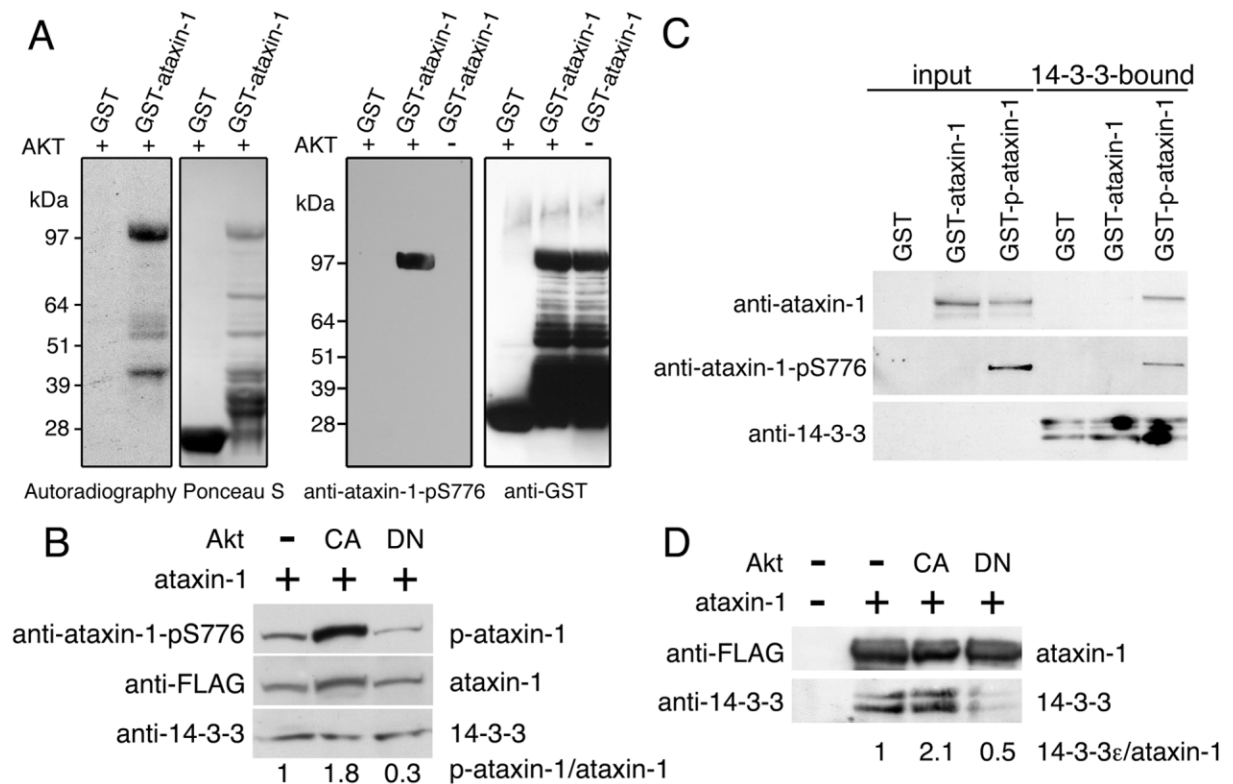
Figure 5. Interaction of Ataxin-1 with 14-3-3 Requires Akt Phosphorylation

(A) Akt phosphorylates ataxin-1 at S776 in vitro. Assays were performed using purified Akt1 kinase and bacterial GST or GST-ataxin-1[30Q] as substrates. Ponceau S staining (left 2 panels), and immunoblotting with anti-ataxin-1-pS776 or anti-GST antibodies (right 2 panels) are shown.

(B) Akt phosphorylates ataxin-1 at S776 in vivo. HeLa cells were cotransfected with FLAG- ataxin-1[2Q]-S776 and either constitutively active (CA-Akt), dominantly negative (DN-Akt) forms of Akt1, or a control plasmid (−). Immunoblotting with anti-ataxin-1-pS776, anti-FLAG, or anti-14-3-3ζ antibodies revealed the S776-phosphorylated ataxin-1 (p-ataxin-1), total ataxin-1, or 14-3-3ζ respectively. The relative ratios of the S776-phosphorylated ataxin-1 to total ataxin-1 are shown.

(C) Ataxin-1 binding to 14-3-3 requires Akt phosphorylation. Immunopurified 14-3-3 was incubated with either GST, unphosphorylated GST-ataxin-1, or Akt1-phosphorylated GST-ataxin-1 (GST-p-ataxin-1). GST-fused proteins (input) and the 14-3-3-bound proteins were resolved by SDS-PAGE and immunoblotted with anti-ataxin-1, anti-ataxin-1-pS776, or mixture of anti-14-3-3ε and anti-14-3-3ζ antibodies.

(D) Akt phosphorylation regulates 14-3-3 binding to ataxin-1 in vivo. HeLa cells were cotransfected with FLAG-ataxin-1[2Q] and either CA-Akt, DN-Akt, or a control plasmid (−). Lysates were immunoprecipitated with anti-FLAG antibodies. Similar amounts of ataxin-1 immunoprecipitates were resolved by SDS-PAGE and immunoblotted with anti-FLAG or mixtures of anti-14-3-3ε and anti-14-3-3ζ antibodies. Relative signal ratios of coimmunoprecipitated 14-3-3ε to ataxin-1 are shown below.

vitro binding assay. Bacterially expressed GST or GST-ataxin-1[30Q] were purified to homogeneity and incubated with purified 14-3-3 proteins that were immobilized on antibody-conjugated agarose. Ataxin-1 associated with 14-3-3 only when ataxin-1 was phosphorylated with Akt1 kinase (Figure 5C). We next cotransfected HeLa cells with ataxin-1[2Q] and either CA-Akt or DN-Akt and carried out immunoprecipitation on lysates from these cells to pull down ataxin-1 protein complexes. Because ataxin-1 levels varied with Akt1 coexpression (Figure 5B), the amounts of immunoprecipitates resolved in SDS-PAGE were adjusted according to the levels of ataxin-1 to have a similar amount of immunoprecipitated ataxin-1 in each lane (Figure 5D). Coimmunoprecipitation of 14-3-3 was increased in transfectants with ataxin-1 and CA-Akt (Figure 5D); this could not be attributed to changes in the endogenous levels of 14-3-3 proteins, which were similar in all cells (Figure 5B and data not shown). On the other hand, coimmunoprecipitation of 14-3-3 was significantly decreased in

transfectants coexpressing ataxin-1 and DN-Akt (Figure 5D). This result suggests that ataxin-1 association with 14-3-3 is regulated by Akt kinases in vivo.

Phosphatidylinositol 3-Kinase/Akt Pathway Modulates Ataxin-1-Induced Neurodegeneration

Knowing that Akt kinase regulates the binding of ataxin-1 to 14-3-3, we postulated that Akt kinase might modulate ataxin-1-induced degeneration. To test this hypothesis, we crossed SCA1[82Q] flies with flies overexpressing Drosophila Akt1 (dAkt1) under the control of the gmr-GAL4 driver. Flies overexpressing dAkt1 alone exhibited slightly enlarged eyes and a mild disruption of the regular, external lattice, as previously described (Verdu et al., 1999; Figure 6A, panels 1 and 2). SCA1[82Q]/dAkt1 double transgenic flies showed profoundly disorganized ommatidia and numerous necrotic spots (Figure 6A, panel 6, see inset), a much more severe phenotype than found in flies expressing dAkt1 or ataxin-1[82Q]
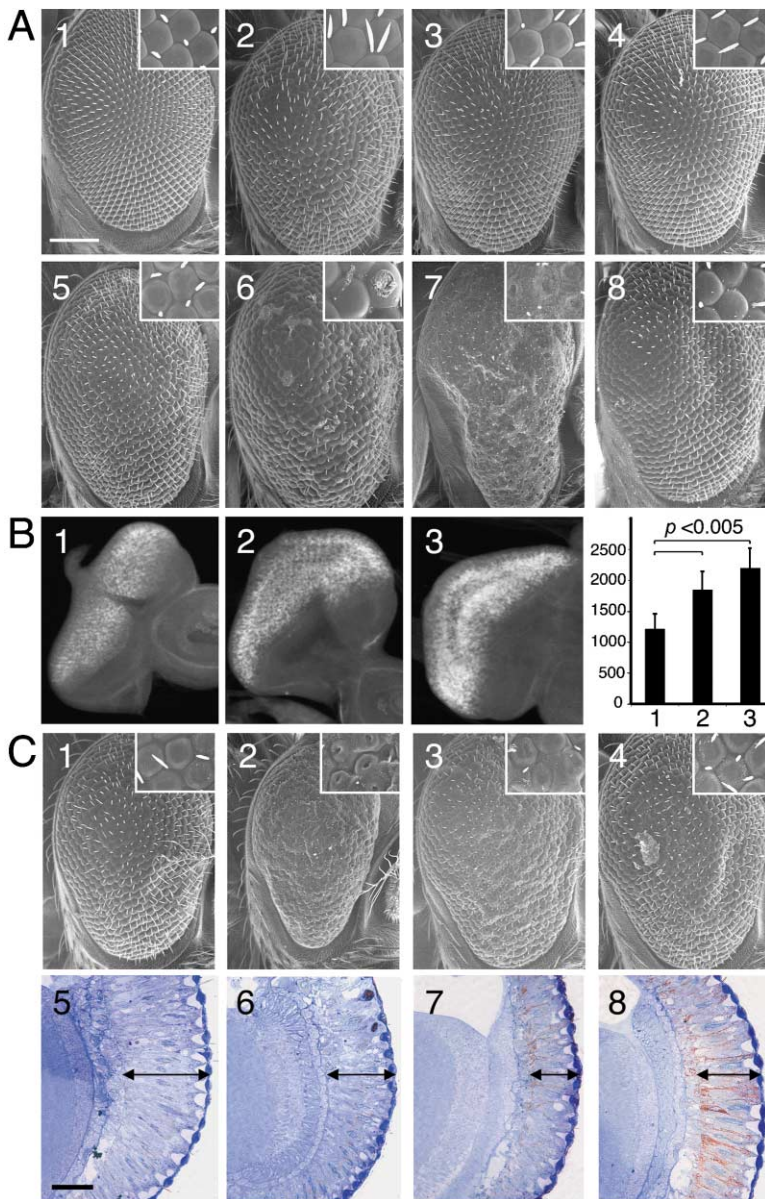
Figure 6. PI3K/Akt Signaling Modulates Ataxin-1-Induced Neurodegeneration in Flies

(A) Akt and PI3K promote ataxin-1-induced neurodegeneration. Shown are SEM eye images of a control fly eye (*gmr-GAL4/+*, panel 1) or fly eyes expressing dAkt1 (*UAS-dAkt1/gmr-GAL4*, panel 2), dPI3K (*UAS-dPI3K/gmr-GAL4*, panel 3), dPDK1 (*dPDK1^EP(3)3553^/gmr-GAL4*, panel 4), ataxin-1[82Q] (*UAS-SCA1^82Q^[F7]/gmr-GAL4*, panel 5) alone, ataxin-1[82Q] together with dAkt1 (*UAS-SCA1^82Q^[F7]/UAS-dAkt1/gmr-GAL4*, panel 6), dPI3K (*UAS-SCA1^82Q^[F7]/UAS-dPI3K/gmr-GAL4*, panel 7), or dPDK1 (*UAS-SCA1^82Q^[F7]/dPDK1^EP(3)3553^/gmr-GAL4*, panel 8). All flies were raised at 23°C. Scale bar: 100 μm. Insets show a higher magnification of ommatidia field.

(B) Akt and PI3K induce ataxin-1 protein accumulation. Immunofluorescence staining of larval eye discs from flies expressing ataxin-1[82Q] alone (*elav-GAL4 UAS-SCA1^82Q^[F7]/+*, panel 1), ataxin-1[82Q] together with dAkt1 (*elav-GAL4 UAS-SCA1^82Q^[F7]/UAS-dAkt1*, panel 2) or dPI3K (*elav-GAL4 UAS-SCA1^82Q^[F7]/UAS-dPI3K*, panel 3) with anti-ataxin-1 antibodies (11750VII). Semi-quantification of fluorescence signals (in arbitrary units) from each transgenic fly is provided in right panel (n = 7). Ataxin-1 staining was significantly stronger in flies coexpressing dAkt or dPI3K ($p < 0.005$).

(C) Modulation of ataxin-1 neurodegeneration by Akt1 is dosage dependent.

Shown are SEM eye images (panels 1 and 2) and eye sections (panels 5 and 6) of sibling male flies expressing ataxin-1[82Q] (*UAS-SCA1^82Q^[F7]/Tp(3;Y)L58/gmr-GAL4*, panels 1 and 5), or ataxin-1[82Q] with a chromosomal duplication of dAkt1 (*UAS-SCA1^82Q^[F7]/Dp(3:Y)L58/gmr-GAL4*, panels 2 and 6) and raised at 23°C. Transgenic flies expressing ataxin-1[82Q] (*UAS-SCA1^82Q^[F7]/gmr-GAL4*, panels 3 and 7) or ataxin-1[82Q] and heterozygous for a loss-of-function allele of *dAkt1* (*UAS-SCA1^82Q^[F7]/gmr-GAL4/dAkt1^0422^*, panels 4 and 8) were raised at 26.5°C and their SEM eye images (panels 3 and 4) and eye sections (panels 7 and 8) are shown. Insets (panels 1–4) show a higher magnification of ommatidia field. Arrows indicate retinal thickness (panels 5–8). Scale bar: 50 μm.

alone (Figure 6A, panels 2 and 5). Eye sections of these flies revealed a severely disorganized retina with deformed or missing rhabdomeres (data not shown). Akt overexpression clearly exacerbates ataxin-1 toxicity.

Akt is a component of the phosphatidylinositol 3-kinase (PI3K)/Akt signaling pathway (Cantley, 2002). To investigate the possible role of PI3K/Akt signaling in SCA1 pathogenesis, we crossed the *SCA1^82Q^* flies with flies overexpressing either *Drosophila* PI3K (dPI3K) or phosphoinositide-dependent kinase-1 (dPDK1), two signaling components upstream of Akt known to regulate cell size in *Drosophila*. We also evaluated the effect of glycogen synthase kinase 3 (dGSK3), a downstream effector of Akt. All these transgenes were expressed under the control of the *gmr-GAL4* driver. Similar to dAkt1, overexpression of dPI3K and dPDK1 increased the ommatidia and eye size, but none of them, including

dGSK3, caused severe disorganization on their own (Figure 6A, panels 3 and 4, and data not shown). Strikingly, overexpression of dPI3K dramatically worsened ataxin-1 neurodegeneration (Figure 6A, panel 7), while neither dPDK1 nor dGSK3 had a significant effect (Figure 6A, panel 8, and data not shown). Ataxin-1 levels were significantly increased by coexpression of dAkt1 or dPI3K as detected by immunofluorescence staining of larval eye discs (Figure 6B). This observation is consistent with our findings that Akt induced ataxin-1 accumulation in transfected cells by enhancing the binding of ataxin-1 to 14-3-3 (Figures 5B and 5D). Interestingly, ataxin-1 levels are significantly higher in flies coexpressing dPI3K than in those coexpressing dAkt1 ($p < 0.05$), correlating with the more pronounced degeneration caused by dPI3K (Figure 6B and Figure 6A, panel 7 compared with panel 6). These data demonstrate that

PI3K/Akt signaling leads to mutant ataxin-1 accumulation and augments ataxin-1-induced neurodegeneration.

To further investigate the role of Akt in modulating the SCA1 phenotype, we crossed SCA1[82Q] flies with flies bearing either a chromosomal duplication of dAkt1 or a loss-of-function allele of dAkt1 (neither of which caused degeneration on their own [data not shown]). SCA1[82Q] flies bearing 3 copies of dAkt1 displayed an exacerbated degenerative phenotype (Figure 6C, panels 2 and 6 compared with panels 1 and 5). The effect of dAkt1 loss-of-function was evaluated in SCA1[82Q] flies raised at a higher temperature (26.5°C) (at which ataxin-1[82Q] itself induces a more severe degenerative phenotype [Figure 6C, panels 3 and 7]). Under this condition, ataxin-1-induced neurodegeneration was less severe in SCA1[82Q] flies heterozygous for a loss-of-function allele of dAkt1 (Figure 6C, panels 4 and 8). Stronger suppression of the SCA1 phenotype was observed in flies homozygous for a hypomorphic loss-of-function dAkt1 allele, although those flies were also smaller due to dAkt1 loss-of-function (Supplemental Figure S1 available at http://www.cell.com/cgi/content/full/113/4/457/DC1). These results demonstrate that dAkt1 modulates the ataxin-1-induced neurodegeneration in a dosage-dependent manner. The suppression of the SCA1 phenotype by dAkt1 loss-of-function is particularly important in that it allows us to rule out potential effects caused by protein overexpression. Moreover, it raises the possibility that reducing the activity of Akt kinases might suppress SCA1 pathology and hold therapeutic value.

Discussion

Although polyglutamine expansion is itself pathogenic, the toxicity of mutant ataxin-1 is modulated by several cis-/trans-acting factors. Components of the protein folding and ubiquitin-proteasome pathways, such as chaperones and Ube3a ligase, are trans-acting modulators for ataxin-1's toxicity in cells, flies, and mice (reviewed in Zoghbi and Botas, 2002). A recently discovered cis-acting factor is serine 776, which is phosphorylated in vivo (Emamian et al., 2003). An S776A mutation abolished the ability of ataxin-1[82Q] to induce neurodegeneration in transgenic mice even when ataxin-1 harbored an expanded polyglutamine tract and was localized to the nucleus (Emamian et al., 2003). This finding underscored the role of S776 in SCA1 pathogenesis. In this study, we probed the mechanism by which the S776 residue confers toxicity onto ataxin-1[82Q]. We found that, upon Akt-dependent phosphorylation, S776 mediates the interaction of ataxin-1 with 14-3-3.

14-3-3 Modulates SCA1 Pathogenesis by Stabilizing Ataxin-1

14-3-3 proteins bind to phosphopeptide motifs in a variety of cellular proteins to regulate diverse biological processes such as signal transduction, cell cycle control, and apoptosis (Fu et al., 2000). The function of 14-3-3 binding to ataxin-1 remains unclear, since the cellular function of ataxin-1 is not well understood. The present study does, however, shed light on the mechanism by which 14-3-3 renders ataxin-1 more toxic to neurons.

Previous studies have revealed that 14-3-3 can protect its target protein from proteolysis and dephosphorylation (Tzivion and Avruch, 2002). For example, 14-3-3 stabilizes the nicotinic receptor α4 subunit, elevating its steady-state protein levels (Jeanclos et al., 2001). In this study, we found that 14-3-3 binds and stabilizes ataxin-1 and promotes its accumulation in both transfected cells and transgenic flies. The ataxin-1/14-3-3 interaction might directly stabilize a conformation of ataxin-1 that resists degradation or it might impede access to other ataxin-1-interacting proteins that would facilitate protein clearance. Note that 14-3-3 interacts not only with the expanded mutant ataxin-1 but also the unexpanded wild-type protein. It is therefore possible that 14-3-3 regulates ataxin-1's clearance under physiological conditions. This regulation becomes problematic upon CAG repeat expansion, since longer polyglutamine tracts enhance ataxin-1's interaction with 14-3-3, further stabilizing the mutant protein.

14-3-3 in SCA1 Pathogenesis

We found that 14-3-3 promoted the accumulation of ataxin-1 and also enhanced aggregate formation. The finding that 14-3-3 aggravates SCA1 pathogenesis together with data by Emamian et al. (2003) showing the absence of nuclear inclusions and neuronal dysfuction in mice overexpressing ataxin-1[82Q]-A776 might resurrect the old question of whether nuclear inclusions cause SCA1 pathogenesis, but when ataxin-1 is expressed at physiologic levels, under control of endogenous promoter, neuronal dysfunction occurs in the absence of visible nuclear inclusions (Watase et al., 2002). The absence of nuclear inclusions in ataxin-1[82Q]-A776 mice most likely resulted from efficient clearance of the mutant protein due to its lack of interaction with 14-3-3.

To investigate the possibility that sequestration of 14-3-3 with mutant ataxin-1 interferes with the cellular functions of 14-3-3, we evaluated the effects of 14-3-3 overexpression on the SCA1 phenotype in vivo and found no evidence that loss of 14-3-3 cellular functions plays a major role in SCA1 pathogenesis. If SCA1 pathology was caused simply by sequestration of 14-3-3 by ataxin-1, one would expect exogenous 14-3-3 to suppress the phenotype—yet overexpression of 14-3-3 in SCA1 flies aggravated degeneration. In fact, immunolabeling of cerebellar sections from transgenic mice overexpressing ataxin-1[82Q]-S776 revealed that the distribution of 14-3-3 remains grossly unchanged without sequestration into nuclear inclusions (data not shown); the colocalization of the two proteins to inclusions in cell cultures could be modulated by differences in other cellular proteins or the nature of inclusions (formed over hours in cells versus days and weeks in mice). It is likely that 14-3-3 and ataxin-1 preferentially form soluble protein complexes in vivo, whereby only a minor fraction of 14-3-3 is present in nuclear aggregates.

Consistent with the notion that polyglutamine expansion confers some toxic gain-of-function onto the host protein (Zoghbi and Orr, 2000), we found that larger polyglutamine expansions in ataxin-1 have a higher affinity for 14-3-3. 14-3-3 is able to stabilize wild-type
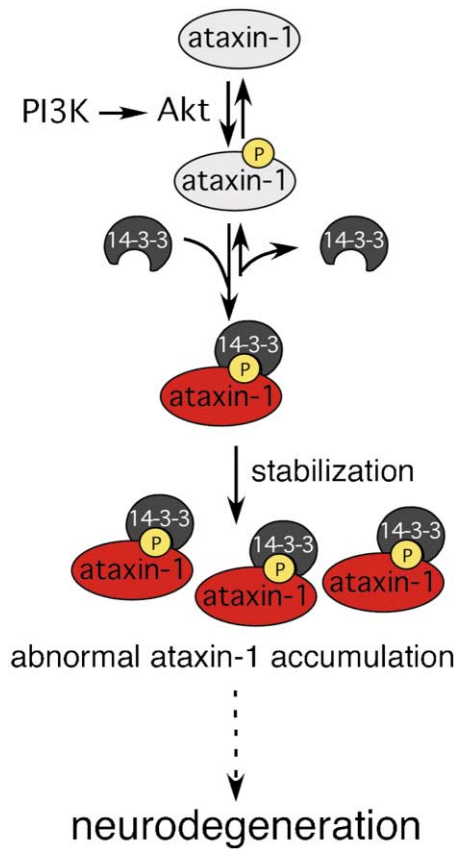
Figure 7. Model Depicting a Mechanism Contributing to Ataxin-1-Induced Neurodegeneration

Akt phosphorylation of ataxin-1 at S776 allows 14-3-3 binding, which stabilizes ataxin-1 perhaps by competing with factors mediating its degradation. The 14-3-3-bound mutant ataxin-1 gradually accumulates and causes neurodegeneration.

ataxin-1, however, and overexpression of 14-3-3 in SCA1[30Q] flies enhanced the neurotoxicity of ataxin-1[30Q] (data not shown). These observations are consistent with the proposed role for 14-3-3 in stabilizing ataxin-1 (Figure 7). The neurotoxic effects of mutant ataxin-1 are likely to be more pronounced in cells expressing high levels of 14-3-3. Many of the 14-3-3 isoforms are abundantly expressed in brain tissue, with different expression patterns for each cell-type; isoforms β, γ, and η are particularly abundant in Purkinje cells (Baxter et al., 2002), which suffer the most severe degeneration. High expression levels of certain 14-3-3 isoforms could contribute to the selective neuronal vulnerability characteristic of SCA1.

14-3-3 and Human Neurodegenerative Disorders

Previous studies have found links between 14-3-3 and other human neurodegenerative disorders. The neurofibrillary tangles in AD are composed primarily of hyperphosphorylated tau proteins (Lee et al., 2001) and contain 14-3-3 (Layfield et al., 1996), which modulates tau phosphorylation (Hashiguchi et al., 2000). Whether this interaction stabilizes tau remains to be determined. In PD, 14-3-3 is detectable in Lewy bodies, which accumu-

late α-synuclein (Kawamoto et al., 2002). Interestingly, α-synuclein shares sequence homology with 14-3-3 and binds both to 14-3-3 and to some 14-3-3 binding partners (Ostrerova et al., 1999). This finding suggests a possible role for either 14-3-3 or 14-3-3 binding proteins in α-synuclein-induced pathology. Moreover, 14-3-3 was recently found to associate with α-synuclein in a soluble protein complex that mediates dopamine-dependent neurotoxicity (Xu et al., 2002). It would be interesting to determine whether 14-3-3 plays any role in stabilizing α-synuclein. When searching for consensus 14-3-3 binding motifs in other polyglutamine-containing proteins, we found the RXXSXP motif in ataxin-2, α1A subunit voltage-gated calcium channel, ataxin-7, and atrophin-1. Further studies are necessary to determine if there is an interaction between these proteins and 14-3-3 and whether such interactions affect the pathogenesis of SCA2, SCA6, SCA7, and DRPLA, respectively.

PI3K/Akt Signaling and Neurodegeneration

Akt phosphorylates ataxin-1 and promotes its binding to 14-3-3, which in turn leads to ataxin-1 accumulation and neurodegeneration (Figure 7). Loss of dAkt1 function suppressed ataxin-1-induced neurodegeneration in a dosage-dependent manner. Akt is activated when recruited to the plasma membrane and phosphorylated at T308 and S473 by PDK1 and a yet-to-be identified "S473-kinase" (Brazil et al. 2002). That dPI3K overexpression aggravates the SCA1 phenotype more than dAkt1 overexpression is consistent with the important role of dPI3K in fully activating the signaling cascade (Figures 6A and 6B). Because dPDK1 overexpresssion is insufficient to promote ataxin-1-induced degeneration, we propose that the "S473-kinase" plays a pivotal role in activating dAkt to modulate ataxin-1's toxicity.

PI3K/Akt signaling is a major pathway mediating survival signals in neuronal cells in response to factors such as insulin-like growth factor 1 (IGF-1; Brunet et al., 2001; Cantley, 2002, Hunter, 2000). Therefore, PI3K/Akt signaling is generally considered neuroprotective, acting against stress conditions that occur during neurodegeneration. IGF-1 is known to activate PI3K/Akt signaling and to protect against neuronal death induced by amyloid-β peptide, a toxic agent in AD (Dore et al., 1997; Wei et al., 2002). Likewise, Akt activation triggered by IGF-1 inhibits neuronal death induced by mutant huntingtin (Humbert et al., 2002).

It is therefore surprising to find that in SCA1 flies, PI3K/Akt promoted ataxin-1-induced neurodegeneration. It is possible that PI3K and Akt triggered survival signaling, as they do in other conditions, but also induced ataxin-1 phosphorylation and thus its interaction with 14-3-3. Whatever survival-promoting effect they exert may be counteracted by the greater neurotoxicity of mutant ataxin-1 accumulation in the cells. It is unlikely that Akt phosphorylation of ataxin-1 was programmed solely as a self-destruction pathway to antagonize cell survival signaling; it is more likely that the physiological activity of ataxin-1 is regulated in accordance with cell survival signaling. The differential effects of PI3K/Akt signaling upon each pathogenic protein exemplify the diversity of cellular responses in different human neurodegenerative

diseases. Activation of PI3K/Akt might have beneficial effects for some neurodegenerative diseases but be deleterious for others. The availability of fly and mouse models for various neurodegenerative disorders will allow in vivo analysis of PI3K/Akt signaling as well as 14-3-3 interactions in various neurodegenerative disorders. Because 14-3-3 proteins are functionally interchangeable in different species (Irie et al., 1994), data obtained in model organisms are likely to prove clinically relevant.

In sum, we have found a mechanism by which PI3K/Akt signaling and 14-3-3 modulate ataxin-1 neurotoxicity. The identification of factors modulating SCA1 pathology may lead to therapeutic interventions such as interfering with ataxin-1/14-3-3 interaction using small peptides or reducing PI3K/Akt signaling by specific kinase inhibitors.

Experimental Procedures

Mammalian Expression Constructs

Plasmids for FLAG-tagged ataxin-1 variants and GFP-ataxin-1 have been described (Cummings et al., 1998; Emamian et al., 2003). 14-3-3ε and 14-3-3ζ cDNAs were C-terminally tagged with haemagglutinin (HA)- and myc-epitopes respectively by PCR (Primer sequences shown in Supplemental Table S1 available online at http://cgi/content/full/113/4/457/DC1). The products were inserted into pIRES2 (Clontech) to make a bi-cistronical expression plasmid pIRES-HA-14-3-3 ε/myc-14-3-3ζ. Myc-14-3-3ζ was subcloned into pcDNA3.1 (Invitrogen). pUSEamp-Akt1 (N-terminal myristoylation) and pUSEamp-Akt1 K179M (Upstate) expressed constitutively active and dominant negative-Akt1.

Immunoprecipitation, Mass Spectrometry, and Western Blotting Analysis

Cell transfections were done by Lipofectamine 2000 (Invitrogen). Whole cell extacts were prepared in RIPA buffer (50 mM Tris-HCl [pH 8.0], 0.15 M NaCl, 1% NP-40, 0.1% SDS, 0.5% sodium deoxycholate, and 5 mM EDTA) supplemented with protease inhibitor cocktail (Sigma) and phosphatase inhibitors (10 mM sodium fluoride and 5 mM sodium orthovanadate). Cells were lysed in TST buffer (50 mM Tris-HCl [pH 7.5], 0.15 M NaCl, and 0.5% Triton X-100) containing protease inhibitors and subjected to immunoprecipitation with either anti-FLAG or anti-HA-conjugated gels (Sigma). The Protein Chemistry Laboratory at Baylor College of Medicine performed mass spectrometry. Polyclonal antibodies against 14-3-3ε and 14-3-3ζ (Santa Cruz), and against β, γ, ε, ζ, and τ isoforms (Baxter et al., 2002) were used. Anti-ataxin-1 antibodies (11750VII) and those against S776-phosphorylated ataxin-1 (PN1168) have been described (Emamian et al., 2003). Other antibodies used: mouse monoclonal anti-HA (BabCo), anti-myc and anti-FLAG (Sigma), anti-GAPDH (Advance immunochemical), rabbit polyclonal anti-FLAG (Sigma), and goat polyclonal anti-GST (Amersham).

In Vitro Phosphorylation and Binding Assays

Ataxin-1[30Q] cDNA was cloned in pGEX-4T1 (Amersham) for GST-ataxin-1 expression. Purified GST-fused proteins were incubated in dilution buffer I (Upstate) supplemented with 75 mM MgCl$_2$, 0.5 mM cold ATP, 10 μCi [γ-P^{32}]ATP, and 0.5 μg recombinant Akt1 (Upstate) at 30°C for 15 min. Reaction products were resolved by SDS-PAGE, transferred onto nitrocellulose membranes and subjected to Ponceau S staining and autoradiography. For immunoblotting with anti-ataxin-1-pS776 antibodies, Akt1 phosphorylation was performed at 30°C for 1 hr in reaction mixtures containing 10 mM cold ATP without [γ-P^{32}]ATP. 14-3-3 proteins were immunoprecipitated with anti-HA agarose from HeLa cells transfected with pIRES-HA-14-3-3ε/myc-14-3-3ζ. Purified GST-fused proteins were incubated with immobilized 14-3-3 in TST buffer at 4°C for 1.5 hr. The 14-3-3 bound proteins were resolved by SDS-PAGE followed by immunoblotting.

Yeast Two-Hybrid Screening

A C-terminal fragment (amino acids 529–816) was PCR amplified (see Supplemental Table S1 at above URL for primer sequences) to generate pGBKT7-ataxin-1C288. Yeast transformants (strain AH109) of pGBKT7-ataxin-1C288 were transformed with plasmids from human brain and spleen cDNA libraries (Clontech). Approximately 1 × 10^6 transformants were screened for growth on medium lacking leucine, tryptophan, histidine, and adenine. Among 126 positive clones, 14-3-3β was identified 6 times, and once for 14-3-3ε. Human 14-3-3ζ and 14-3-3ε cDNAs were inserted in pACT2 (Clontech) and were transformed to AH109 yeasts with pGBKT7-ataxin-1 ([2Q]-S776, [30Q]-S776, [82Q]-S776, or [82Q]-A776) to test for interactions.

Histology, Immunofluorescence Microscopy, and Confocal Microscopy

Eye sections, histological and indirect immunofluorescence stainings were performed as described (Fernandez-Funez et al. 2000). Confocal microscopy was performed using a Zessis LSM 510 microscope. For double labeling, images from the same confocal plane were recorded. Immunofluorescence staining of larval tissues was done with anti-ataxin-1 antibody (11750VII). Ataxin-1 fluorescent signals of eye discs were recorded in Z-stacks of 1 μm thickness by Biorad confocal microscope using the same settings. The Z-stacks were flattened and signal was quantified using ImageJ software. Average signal from seven samples for every genotype was calculated and plotted using Excel software.

Drosophila Genetics

Drosophila 14-3-3ε was inserted in the pUAST vector for generating one *UAS-d14-3-3ε* transgenic line. Thirty-two new *UAS-d14-3-3ε* lines were generated by mobilization of the original line with transposase and then crossed with the weak line *SCA1^{82Q}[F7]/gmr-GAL4* at 23°C. The *d14-3-3ε* transgenic lines were classified (weak/strong) based on their ability to produce synthetic lethality over *SCA1^{82Q}*. The null allele *14-3-3ε^{ex4}* was generated by imprecise mobilization of the P element insertion *14-3-3ε^{j2B10}*. Females of the strong *y w UAS-SCA1^{82Q}[N35y]* line crossed with males *y w; UAS-d14-3-3ε/ TM3,Sb* produced slow moving, necrotic larvae *y w UAS-SCA1^{82Q}[N35y]/UAS-d14-3-3ε* and normal siblings *y w UAS-SCA1^{82Q}[N35y]/TM3,Sb* that were dissected and fixed for ataxin-1 detection. Flies of the genotypes *Tp(3;Y)L58, leo^{07103}, dAkt1^{04226}* (Bloomington Stock Center), *UAS-dAkt1* (Verdu et al., 1999), *dPDK1$^{EP(3)3553}$* (Cho et al., 2001), *UAS-dPI3K* (Leevers et al., 1996, Ludwig Institute for Cancer Research), *y w; UAS-d14-3-3ε, y w; UAS-d14-3-3ε(9 or)* or *14-3-3ε^{ex4}* were crossed with *y w UAS-SCA1^{82Q}[F7]; gmr-GAL4* (Fernandez-Funez et al., 2000), or *gmr-GAL4* alone as control for adult eye analysis, or *elav-GAL4 UAS-SCA1^{82Q}[F7]* for ataxin-1 quantification in larval eye disc. All crosses incubated at 23°C, except crosses with *dAkt1^{04226}* (26.5 and 27°C) and *14-3-3ε^{ex4}* and *leo^{07103}* (27.5°C). Adult flies were dehydrated in 100% ethanol and prepared for scanning electron microscopic (SEM) analysis of the eyes.

References

Baxter, H.C., Liu, W.G., Forster, J.L., Aitken, A., and Fraser, J.R. (2002). Immunolocalisation of 14–3-3 isoforms in normal and scrapie-infected murine brain. Neuroscience *109*, 5–14.

Brazil, D.P., Park, J., and Hemmings, B.A. (2002). PKB binding proteins. Getting in on the Akt. Cell *111*, 293–303.

Brunet, A., Datta, S.R., and Greenberg, M.E. (2001). Transcription-dependent and -independent control of neuronal survival by the PI3K-Akt signaling pathway. Curr. Opin. Neurobiol. *11*, 297–305.

Brunet, A., Kanai, F., Stehn, J., Xu, J., Sarbassova, D., Frangioni, J.V., Dalal, S.N., DeCaprio, J.A., Greenberg, M.E., and Yaffe, M.B. (2002). 14–3-3 transits to the nucleus and participates in dynamic nucleocytoplasmic transport. J. Cell Biol. *156*, 817–828.

Cantley, L.C. (2002). The phosphoinositide 3-kinase pathway. Science *296*, 1655–1657.

Cho, K.S., Lee, J.H., Kim, S., Kim, D., Koh, H., Lee, J., Kim, C., Kim, J., and Chung, J. (2001). Drosophila phosphoinositide-dependent kinase-1 regulates apoptosis and growth via the phosphoinositide 3-kinase-dependent signaling pathway. Proc. Natl. Acad. Sci. USA *98*, 6144–6149.

Cummings, C.J., Mancini, M.A., Antalffy, B., DeFranco, D.B., Orr, H.T., and Zoghbi, H.Y. (1998). Chaperone suppression of aggregation and altered subcellular proteasome localization imply protein misfolding in SCA1. Nat. Genet. *19*, 148–154.

Dawson, T., Mandir, A., and Lee, M. (2002). Animal models of PD: pieces of the same puzzle? Neuron *35*, 219–222.

Dore, S., Kar, S., and Quirion, R. (1997). Insulin-like growth factor I protects and rescues hippocampal neurons against beta-amyloid- and human amylin-induced toxicity. Proc. Natl. Acad. Sci. USA *94*, 4772–4777.

Emamian, E.S., Kaytor, M.D., Duvick, L.A., Zu, T., Tousey, S.K., Clark, H.B., Zoghbi, H.Y., and Orr, H.T. (2003). Serine 776 of ataxin-1 is critical for polyglutamine-induced disease in *SCA1* transgenic mice. Neuron *38*, 375–387.

Fernandez-Funez, P., Nino-Rosales, M.L., de Gouyon, B., She, W.C., Luchak, J.M., Martinez, P., Turiegano, E., Benito, J., Capovilla, M., Skinner, P.J., et al. (2000). Identification of genes that modify ataxin-1-induced neurodegeneration. Nature *408*, 101–106.

Fu, H., Subramanian, R.R., and Masters, S.C. (2000). 14–3-3 proteins: structure, function, and regulation. Annu. Rev. Pharmacol. Toxicol. *40*, 617–647.

Hashiguchi, M., Sobue, K., and Paudel, H.K. (2000). 14–3-3ζ is an effector of tau protein phosphorylation. J. Biol. Chem. *275*, 25247–25254.

Humbert, S., Bryson, E.A., Cordelieres, F.P., Connors, N.C., Datta, S.R., Finkbeiner, S., Greenberg, M.E., and Saudou, F. (2002). The IGF-1/Akt pathway is neuroprotective in Huntington's disease and involves Huntingtin phosphorylation by Akt. Dev. Cell *2*, 831–837.

Hunter, T. (2000). Signaling–2000 and beyond. Cell *100*, 113–127.

Irie, K., Gotoh, Y., Yashar, B.M., Errede, B., Nishida, E., and Matsumoto, K. (1994). Stimulatory effects of yeast and mammalian 14–3-3 proteins on the Raf protein kinase. Science *265*, 1716–1719.

Jackson, G.R., Wiedau-Pazos, M., Sang, T.K., Wagle, N., Brown, C.A., Massachi, S., and Geschwind, D.H. (2002). Human wild-type tau interacts with wingless pathway components and produces neurofibrillary pathology in Drosophila. Neuron *34*, 509–519.

Jeanclos, E.M., Lin, L., Treuil, M.W., Rao, J., DeCoster, M.A., and Anand, R. (2001). The chaperone protein 14–3-3eta interacts with the nicotinic acetylcholine receptor alpha 4 subunit. Evidence for a dynamic role in subunit stabilization. J. Biol. Chem. *276*, 28281–28290.

Kawamoto, Y., Akiguchi, I., Nakamura, S., Honjyo, Y., Shibasaki, H., and Budka, H. (2002). 14–3-3 proteins in Lewy bodies in Parkinson disease and diffuse Lewy body disease brains. J. Neuropathol. Exp. Neurol. *61*, 245–253.

Kaytor, M.D., and Warren, S.T. (1999). Aberrant protein deposition and neurological disease. J. Biol. Chem. *274*, 37507–37510.

Layfield, R., Fergusson, J., Aitken, A., Lowe, J., Landon, M., and

Mayer, R.J. (1996). Neurofibrillary tangles of Alzheimer's disease brains contain 14-3-3 proteins. Neurosci. Lett. *209*, 57–60.

Lee, V.M., Goedert, M., and Trojanowski, J.Q. (2001). Neurodegenerative tauopathies. Annu. Rev. Neurosci. *24*, 1121–1159.

Leevers, S.J., Weinkove, D., MacDougall, L.K., Hafen, E., and Waterfield, M.D. (1996). The Drosophila phosphoinositide 3-kinase Dp110 promotes cell growth. EMBO J. *15*, 6584–6594.

Lucas, J.J., Hernandez, F., Gomez-Ramos, P., Moran, M.A., Hen, R., and Avila, J. (2001). Decreased nuclear beta-catenin, tau hyperphosphorylation and neurodegeneration in GSK-3beta conditional transgenic mice. EMBO J. *20*, 27–39.

Nakamura, K., Jeong, S.Y., Uchihara, T., Anno, M., Nagashima, K., Nagashima, T., Ikeda, S., Tsuji, S., and Kanazawa, I. (2001). SCA17, a novel autosomal dominant cerebellar ataxia caused by an expanded polyglutamine in TATA-binding protein. Hum. Mol. Genet. *10*, 1441–1448.

Ostrerova, N., Petrucelli, L., Farrer, M., Mehta, N., Choi, P., Hardy, J., and Wolozin, B. (1999). α-Synuclein shares physical and functional homology with 14–3-3 proteins. J. Neurosci. *19*, 5782–5791.

Tzivion, G., and Avruch, J. (2002). 14–3-3 proteins: active cofactors in cellular regulation by serine/threonine phosphorylation. J. Biol. Chem. *277*, 3061–3064.

Verdu, J., Buratovich, M.A., Wilder, E.L., and Birnbaum, M.J. (1999). Cell-autonomous regulation of cell and organ growth in Drosophila by Akt/PKB. Nat. Cell Biol. *1*, 500–506.

Watase, K., Weeber, E.J., Xu, B., Antalffy, B., Yuva-Paylor, L., Hashimoto, K., Kano, M., Atkinson, R., Sun, Y., Armstrong, D.L., et al. (2002). A long CAG repeat in the mouse Sca1 locus replicates SCA1 features and reveals the impact of protein solubility on selective neurodegeneration. Neuron *34*, 905–919.

Wei, W., Wang, X., and Kusiak, J.W. (2002). Signaling events in amyloid beta-peptide-induced neuronal death and insulin-like growth factor I protection. J. Biol. Chem. *277*, 17649–17656.

Xu, J., Kao, S.Y., Lee, F.J., Song, W., Jin, L.W., and Yankner, B.A. (2002). Dopamine-dependent neurotoxicity of α-synuclein: a mechanism for selective neurodegeneration in Parkinson disease. Nat. Med. *8*, 600–606.

Yaffe, M.B., Leparc, G.G., Lai, J., Obata, T., Volinia, S., and Cantley, L.C. (2001). A motif-based profile scanning approach for genome-wide prediction of signaling pathways. Nat. Biotechnol. *19*, 348–353.

Zoghbi, H.Y., and Botas, J. (2002). Mouse and fly models of neurodegeneration. Trends Genet. *18*, 463–471.

Zoghbi, H.Y., and Orr, H.T. (2000). Glutamine repeats and neurodegeneration. Annu. Rev. Neurosci. *23*, 217–247.